RECENT ORIGIN OF THE SOLAR SYSTEM DUST BANDS

David Nesvorný, William F. Bottke, Harold F. Levison, and Luke Dones
Southwest Research Institute, 1050 Walnut Street, Suite 400, Boulder, CO 80302; davidn@boulder.swri.edu

ABSTRACT

Infrared Astronomical Satellite (*IRAS*) observations in 1983 revealed the existence of several solar system dust bands. These dust bands are believed to be debris produced by recent disruption events among main-belt asteroids, particularly because dust particles have short dynamical and collisional lifetimes. Using young asteroid families as tracers of recent disruptions in the main belt, we linked the most prominent *IRAS* dust bands with their sources. We propose that the source regions of the dust bands with inclination $9°35$ and $2°1$ are the Veritas asteroid family at 3.17 AU and the Karin cluster located inside the Koronis asteroid family at 2.865 AU, respectively. The Veritas family and the Karin cluster formed by collisional disruptions of their ~ 140 and ~ 25 km diameter parent bodies at 8.3 ± 0.5 and 5.8 ± 0.2 Myr ago, respectively. Asteroid material from the former source may represent about one-quarter of the interplanetary dust particles that have been collected in the Earth's stratosphere (and that have been extensively studied in laboratories). We were unable to identify a recent collision in the main-belt region that could be responsible for the $1°4$ *IRAS* dust band. The region of the Themis family remains the best candidate for this dust band. We speculate that the (4652) Iannini cluster ($\lesssim 5$ Myr old, $\sim 12°$ inclination) is the source for the J/K dust band and that the (1521) Seinajoki cluster ($\sim 15°$ inclination) is the ultimate source for the M/N dust band. We point out that the dust bands' spatial distributions are consistent with our proposed sources. This, and the fact that many prominent but ancient asteroid families have no associated dust bands, strongly suggests that dust bands are primarily by-products of recent asteroid breakup events that occur throughout the main belt.

Subject headings: infrared: solar system — interplanetary medium — minor planets, asteroids

1. INTRODUCTION

A substantial fraction of the dust that reaches Earth was produced by collisions in the main belt (e.g., Dermott et al. 2002). An important goal of asteroid science is to link particular dust particles captured in the upper atmosphere to their distant parent bodies. By doing so, we can combine cosmochemical information obtained from our dust collections with remote asteroid observations, ultimately producing the equivalent of multiple asteroid sample return missions (on the cheap). To do this, however, we first need to understand the dynamical processes and evolutionary pathways that deliver dust from the main belt to the Earth.

Disruptive collisions in the main-belt region can liberate fragments from parent bodies that range in size from dust grains tens of microns in diameter to sizable asteroids (e.g., Davis et al. 1979). Because the ejection velocities of large fragments are generally small compared to their orbital velocities (Hirayama 1918; Fujiwara et al. 1989; Nakamura, Suguiyama, & Fujiwara 1992; Michel et al. 2001; Davis et al. 2002; Holsapple et al. 2002), most start with nearly identical orbits. Conversely, dust particles can be spurted out at high velocities that may be as high as several kilometers per second (Vickery 1993).

The dynamical evolution of an individual fragment depends strongly on its diameter. For example, while meter-sized and larger bodies are readily spread into a dispersed toroid around the Sun via planetary perturbations, smaller bodies, such as ~ 5–100 μm dust particles, have their dynamical evolution dominated by nongravitational forces such as Poynting-Robertson and solar wind drag (Burns, Lamy, & Soter 1979; Dermott et al. 2002). These mechanisms compel dust particles to spiral inward toward the Sun. Once the dust particles reach $\lesssim 2$ AU, strong secular resonances and

encounters with the terrestrial planets increase the latitudinal spread of the evolving dust cloud (Kehoe, Dermott, & Grogan 2001). Eventually, some fraction of dust grains produced by asteroid collisions fall into the Sun, impact the Earth's atmosphere, or are accreted by other terrestrial planets. The net dynamical lifetime of ~ 5–100 μm particles from source to sink is believed to be $\sim 10^5$–10^6 yr (Burns et al. 1979).

The evolution of debris produced by an asteroid collision starts almost immediately. Meter-sized and larger fragments erode or become disrupted by collisions with background asteroids (e.g., Marzari, Davis, & Vanzani 1995). Dust particles are comminuted by collisions with background interplanetary dust particles (IDPs), both cometary and asteroidal in origin (Grün et al. 1985; see also Love & Brownlee 1993). In effect, mass is being continuously redistributed into smaller fragments via a collisional cascade. Moreover, because submicron dust grains can be ejected from the solar system by radiation pressure (Zook & Berg 1975), mass is removed at the small-particle end. Hence, and because the asteroid dust grains are also lost by impacts into the Sun and terrestrial planets, the total cross-sectional area of dust produced by an asteroid breakup declines with time (Sykes & Greenberg 1986; Grogan, Dermott, & Durda 2001).

This scenario is supported by the following observational evidence:

1. The large observable fragments of the disrupted body are expected to group at similar orbital locations. To identify these groups, researchers (starting with Hirayama 1918) look for clusters of asteroid positions in the space of so-called proper orbital elements: the proper semimajor axis

(a_P), proper eccentricity (e_P), and proper inclination (i_P). The orbital elements describe the size, shape, and tilt of orbits. Proper orbital elements, being more constant over time than instantaneous orbital elements (see Milani & Knežević 1994), provide a dynamical criterion of whether or not a group of bodies has a common ancestor. Using these methods, ejecta from a few tens of major collisions (that is, asteroid families) have been found in the main-belt region (see Zappalà et al. 1994, 2002).

2. Several solar system dust bands were discovered by the *Infrared Astronomical Satellite* (*IRAS*) as residual features on the broad background infrared emission structure (called the zodiacal cloud; Low et al. 1984; Sykes 1988).[1] These emission features are located at a few roughly constant ecliptic latitudes, while they are spread nearly uniformly over all ecliptic longitudes. Several lines of evidence suggest that the *IRAS* dust bands were produced via asteroidal collisions (Dermott et al. 1984; Sykes & Greenberg 1986). Moreover, dust from other potential sources, such as comets or the interstellar medium, has a distinctive spatial distribution that is not consistent with the *IRAS* dust bands (Low et al. 1984; Sykes et al. 1986).

3. Spectroscopic and mineralogic studies suggest that IDPs, which are collected by airborne impaction collectors in the Earth's stratosphere, may be partly asteroidal in origin (e.g., Keller, Thomas, & McKay 1993; Klöck & Stadermann 1994). Roughly one-third of these IDPs may be sampling material from the *IRAS* dust bands (Dermott et al. 2002).

The relationship between observed asteroid families and the *IRAS* dust bands has been a matter of much debate. On the one side, Dermott et al. (1984) proposed that the dust bands consist of material produced by ongoing collisional grinding of bodies within prominent asteroid families. This scenario is referred to in the literature as the equilibrium model. In this model, a large asteroid family with a (mean) proper inclination value i_P produces a population of dust with infrared emission that is peaked at latitudes $\sim i_P$. In particular, the Eos family was believed to produce the dust band observed at $\sim 10°$ latitudes, while the Koronis and Themis families were believed to produce the central dust bands observed at low latitudes (Dermott et al. 1984; Sykes 1988). On the other hand, Sykes & Greenberg (1986) suggested that the *IRAS* dust bands were produced by stochastic breakups of ~ 10 km diameter asteroids that occurred in the main-belt region within the last several million years. This scenario is referred to in the literature as the nonequilibrium model. It is independent of an association of the dust bands with large asteroid families (Sykes & Greenberg 1986).

A problem with the equilibrium scenario is that the mean proper inclination of the large Eos family ($i_P \sim 10°08$) is significantly greater than the proper inclination of the so-called outer band ($i_P = 9°35$; Grogan et al. 2001; we summarize the properties of the dust bands in § 2). Thus, the dust band is not tracing the orbital element distribution of the Eos family as a whole, as would be expected from the equilibrium model, nor it is consistent with most potential source

bodies in the Eos family. These results have challenged the equilibrium scenario for the dust bands' origin.

Recent work by Nesvorný et al. (2002a) produced supporting evidence for the nonequilibrium model of the *IRAS* dust bands' origins. According to this model, the *IRAS* dust bands were produced by recent disruption events among multikilometer bodies in the main asteroid belt (Sykes & Greenberg 1986; Sykes 1988). These events should have left behind distinct fingerprints in the form of compact asteroid families. Indeed, Nesvorný et al. (2002a) discovered a compact asteroid family inside the Koronis family (the Karin cluster) that formed only 5.8 ± 0.2 Myr ago by the collisional disruption of a ~ 25 km diameter parent body. Both the Karin cluster and the model-derived source of one component of the near-ecliptic dust bands were found to have mean inclinations $i_P \approx 2°1$. In addition, the narrow inclination span of the $2°1$ dust band component ($\sigma_{i_P} \approx 0°04$; Grogan et al. 2001) is consistent with the inclination distribution of the Karin cluster ($\sigma_{i_P} \approx 0°03$).

Motivated by this result, we attempted to identify the sources of all major *IRAS* dust bands by systematically searching for compact asteroid families in the main-belt region. In § 2, we summarize observed properties of the dust bands that help us constrain their source regions. In § 3, we identify recent asteroid breakups that best fit these constraints. Implications of the proposed origin of the solar system dust bands are discussed in § 4.

2. BASIC PROPERTIES OF THE SOLAR SYSTEM DUST BANDS

Asteroid dust bands were first detected by *IRAS* (Low et al. 1984) and were later observed by the *Cosmic Background Explorer* satellite (*COBE*; Spiesman et al. 1995) and by a ground-based telescope (Ishiguro et al. 1999). Synthetic models of the dust bands were developed to fit the observations (Dermott et al. 1984; Sykes 1990; Reach 1992; Reach, Franz, & Weiland 1997; Grogan et al. 2001). Here we use results of the most recent model by Grogan et al. (2001). This model adjusts the dust bands' parameters to match *IRAS* observations in the 12, 25, and 60 μm wavelengths. Grogan et al. (2001) calculate that the mean proper inclination of the source of the so-called outer dust band (or γ-band) is $9°35$ and that the two near-ecliptic bands have sources located at mean proper inclinations of $1°43$ and $2°11$ (α and β bands, respectively; Sykes 1988). These values constrain the location of the source regions in the main belt.

Grogan et al. (2001) estimate that the cross-sectional area of material required to account for the outer dust band's infrared emission is $\approx 4 \times 10^9$ km^2, about 5.7 times more than the combined cross-sectional areas of the dust in the near-ecliptic bands. This factor reflects a comparatively larger amount of dust in the outer dust band. The model-derived cross-sectional areas of the dust bands' material can be used to constrain the size of the disrupted parent asteroids. In total, 25% of the zodiacal cloud may be associated with the outer dust band and 5% with the near-ecliptic bands (Dermott et al. 2002).

Several fainter dust bands also exist. Sykes (1988) identified two possible band pairs at inclinations between the β- and γ-bands (E/F, G/H) and two possible band pairs at inclinations higher than that of the γ-band (J/K, M/N). These, except for E/F, were confirmed by *COBE* observations (Reach et al. 1997). Among these weak signals,

---

[1] The temperature of asteroidal dust grains at 2–3.3 AU places their thermal emission in the infrared part of spectra, which is difficult to observe from ground-based facilities because of the enormous background noise produced by thermal emission from the atmosphere and telescope.

probably the most readily detectable are the J/K dust band located at $i_P \approx 12°$ and the M/N dust band located at $i_P \approx 15°$ (Sykes 1990; Reach et al. 1997). Several researchers investigated the link of the J/K and M/N dust bands to the Eunomia/Io (the Io family identified by Williams 1992 is now considered part of the Eunomia family) and Maria families in the central main belt ($\sim$2.5–2.7 AU), respectively, but found problems with these associations (Sykes 1990; Reach et al. 1997).

3. SOURCE REGIONS OF THE DUST BANDS

The chief geologic process that has affected asteroids in the past has been collisions. Catastrophic collisions have created asteroid families (clusters of asteroids with similar orbital elements) and large amounts of dust. In general, prominent families produced by the disruption of diameter $D > 100$ km bodies are not very numerous; fewer than 20 have been reliably established (Zappalà et al. 1994). Most are thought to be hundreds of millions to billions of years old (see Marzari et al. 1995). These numbers and ages appear to be consistent with results from hydrocode modeling of asteroid collisions (see Benz & Asphaug 1999), which indicate that catastrophic disruption events among $D > 100$ km bodies in the present-day main belt should be rare.

This picture has recently been augmented by detailed dynamical analysis and numerical simulations. It is now understood that families are subject to slow spreading and dispersal via numerous tiny resonances in the main belt (Nesvorný et al. 2002c). Moreover, $D < 20$ km asteroids are moved inward toward the Sun and outward away from the Sun over comparatively long timescales by the Yarkovsky effect; this mechanism provides another means for dispersing families (Bottke et al. 2001; D. Vokrouhlický et al. 2003, in preparation). Therefore, an older family's orbital parameters in (a_P, e_P, i_P) space do not reflect the immediate outcomes of cratering events or catastrophic disruptions. Instead, they reveal how it has been " etched " in (a_P, e_P, i_P) space over long timescales by dynamical diffusion and chaotic resonances. On the other hand, tight clusters in (a_P, e_P, i_P) space should represent young families that have not yet had an opportunity to disperse via dynamical mechanisms.

It has been argued (Sykes & Greenberg 1986) that recent disruptions of small asteroids may have produced much of the asteroidal material that currently contributes to the zodiacal dust cloud. Indeed, Durda & Dermott (1997) showed that individual disruptions of $D \gtrsim 10$ km asteroids produce " spikes " that temporarily dominate the overall dust production in the main belt. These spikes typically have a duration of only a few million years. On longer timescales, the spikes fade back to the background as dust grains evolve out the main belt via the Poynting-Robertson effect (see Burns et al. 1979) or are ejected from the solar system by radiation pressure (Zook & Berg 1975).

Accordingly, we believe that best candidates for the source regions of the *IRAS* dust bands are compact (young) asteroid families that have proper inclinations compatible with the model-derived proper inclinations of the dust bands' sources. For this reason, we systematically searched for such asteroid families in the main belt using modern databases of asteroid proper orbital elements. Figure 1 shows the proper semimajor axis and proper inclination of $\approx$100,000 main-belt asteroids (Milani & Knežević 1994;

Knežević, Lemaitre, & Milani 2002a).[2] The horizontal lines indicate the expected inclinations of the main dust bands' sources (1°43 and 2°11 for central bands, 9°35 for the outer band). Dashed lines are drawn at $i_P = 12°$ and $15°$ to approximately indicate the locations of the J/K and M/N dust bands. We also mark locations of several relevant asteroid families. We present our interpretations below.

3.1. 2°11 *Dust Band*

The 2°11 dust band nicely correlates with the inclination location of the Koronis family—one of the original, large families identified by Hirayama early in the 20th century (Fig. 1). We believe, however, that the 2°11 dust band is not related to the entire Koronis family. The Koronis family is apparently very old ($\sim$2 Gyr; Bottke et al. 2001; note its large semimajor axis dispersion cut by the chaotic 5:2 and 7:3 mean motion resonances with Jupiter), such that the original dust produced by the breakup of the parent body must have been removed by radiation forces within $\lesssim 10^7$ yr after the breakup. Although collisions and dust production never never stop inside a family, the dust produced by the breakup event escapes faster than it can be replenished by collisions. The net effect is that the surface area of the dust steadily declines with time after the initial " spike." Hence, after $\sim$2 Gyr of evolution, the total surface area of the Koronis family has dropped by orders of magnitude (Sykes & Greenberg 1986; Grogan et al. 2001).

Recent work has determined a more likely source for the 2°11 dust band (Nesvorný et al. 2002a), namely, the breakup of a moderate-sized ($D \sim 25$ km) Koronis family member only 5.8 ± 0.2 Myr ago (less than 0.2% the age of the solar system, comparatively " yesterday " in cosmic terms). Because the largest member of this cluster is (832) Karin, this cluster has been named the Karin cluster. Estimates from collision models suggest that main-belt asteroids 25 km or so in diameter are expected to be disrupted once every few Myr (Durda & Dermott 1997). Hence, the Karin cluster breakup is not wholly unexpected. In fact, what we see is probably a remnant of the most recent collisional breakup of a $\gtrsim 25$ km asteroid that occurred in the main-belt region. Note that the Karin cluster ($a_P = 2.866$ AU, $e_P = 0.0445$, $i_P = 2°11$) is hidden in Figure 1 in a densely populated region of the Koronis family (see Fig. 1 in Nesvorný et al. 2002a for a zoom in on the Karin cluster).

An interesting aspect of this discovery is the link between the Karin cluster and the 2°11 dust band. The orbital parameters of the cluster match all basic constraints imposed by observations: it has a 2°1 mean proper inclination and 0°03 inclination dispersion. The Karin cluster's parent asteroid was also large enough to account for the observed cross-sectional area of the 2°11 dust band (Grogan et al. 2001). Based on these arguments, we believe it is likely that the 2°11 dust band is a by-product of the Karin cluster formation event.

3.2. 9°35 *Dust Band*

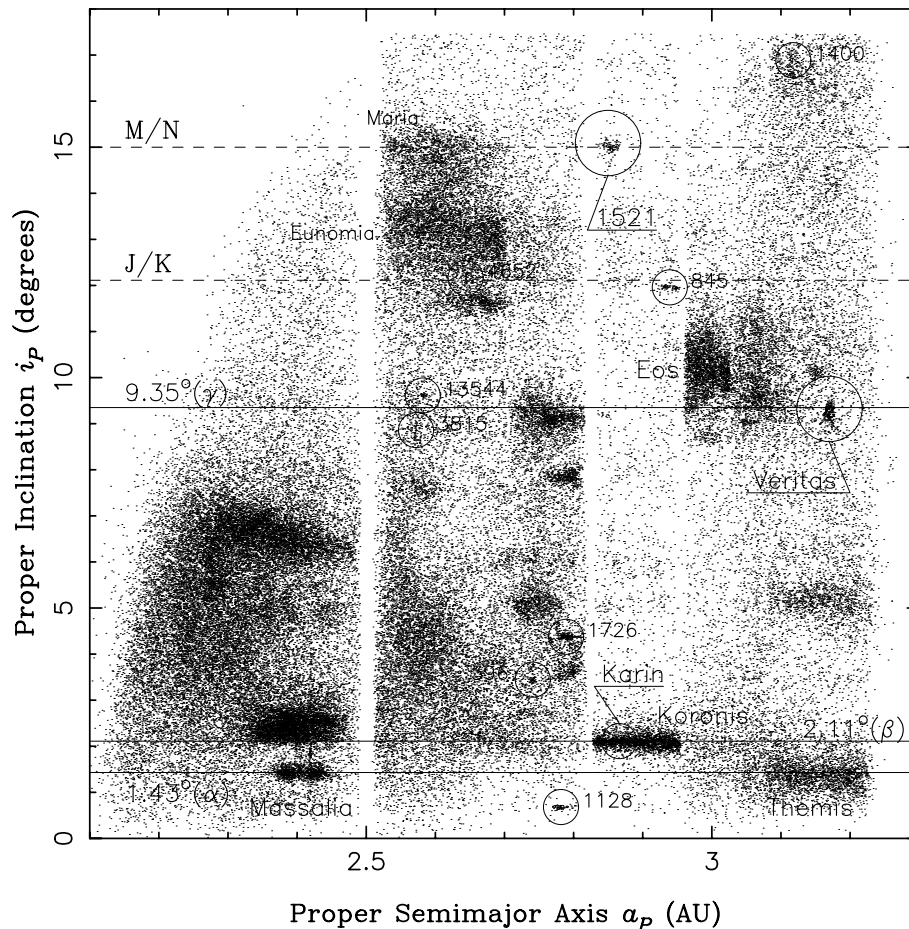We have investigated the origin of the 9°35 dust band. As Figure 1 indicates, the inclinations of the observed Eos

Fig. 1.—Proper semimajor axis and inclination of ≈100,000 main-belt asteroids (Milani & Knežević 1994; Knežević et al. 2002a). Many groups of asteroids with similar proper orbital elements can be readily recognized in the plot. These groups (asteroid families) represent remnants of collisionally disrupted large asteroids. Horizontal lines are drawn at $i_P = 1°43$, $2°11$, $9°35$, $12°$, and $15°$ to indicate the model-derived proper inclination of the *IRAS* dust bands (Sykes 1990; Reach et al. 1997; Grogan et al. 2001). Several relevant asteroid families are denoted. For example, the Veritas family is located at $a_P = 3.17$ AU and $i_P = 9°3$. The Karin cluster (Nesvorný et al. 2002a) is hidden within a densely populated region of the Koronis family. We believe that two of the presently observed solar system dust bands (β and γ) were formed as by-products of recent catastrophic breakups that generated the Veritas family and the Karin cluster. The locations of nine new clusters described in our paper are shown as well (*circles labeled by numbers*; Table 1). We speculate that some of these clusters may be the source regions of the weak dust bands detected by *IRAS* and *COBE* (such as the J/K and M/N dust bands; Sykes 1990; Reach et al. 1997).

family members ($9°5–11°$) are too large to be the source of this dust band. A better fit comes from the more distant Veritas family, which has many observed members with inclinations near $9°35$. Interestingly, the Veritas family is among the most compact in (a_P, e_P, i_P) space of the prominent asteroid families. By modeling the dynamical evolution of bodies in the Veritas family and comparing those results to observations of Veritas family members, some of which reside in powerful resonances, Milani & Farinella (1994) proposed that the Veritas family must be $\lesssim 50$ Myr old. In particular, they found that the largest asteroid in the family, 490 Veritas, would have drifted far away from the rest of the family if it were much older than 50 Myr old. Note that 490 Veritas has only a less than 3% chance of being an interloper. Recently, more refined modeling of the effects of orbital chaos on the structure of the Veritas family has suggested that this family must be even younger ($\lesssim 27$ Myr old; Knežević, Tsiganis, & Varvoglis 2002b).

Figure 2 shows the distribution of proper orbital elements of the Veritas family members. To identify this family, we applied a cluster detection algorithm called the hierarchical

clustering method[3] (HCM; Zappalà et al. 1994; Bendjoya & Zappalà 2002) to a database of 66,089 proper elements (downloaded from the AstDys node in fall 2001; Milani & Knežević 1994; Knežević et al. 2002a) using a cutoff $d_{cutoff} = 40$ m s^{-1}. The orbital structure of the Veritas family is characterized by a tight concentration of family members around asteroid (1086) Nata. This subgroup can be identified with HCM using $d_{cutoff} = 10$ m s^{-1} (the same cutoff was

---

[3] The HCM starts with an individual asteroid position in the proper element space and identifies bodies in its neighborhood with mutual distances less than a threshold limit (so-called cutoff, d_{cutoff}). We define the distance in the (a_P, e_P, i_P) space by

$$d = na_P \left[C_a (\delta a_P / a_P)^2 + C_e (\delta e_P)^2 + C_i (\delta \sin i_P)^2 \right]^{1/2} ,$$

where na_P is the heliocentric velocity of an asteroid on a circular orbit having the semimajor axis a_P; $\delta a_P = |a_P^{(1)} - a_P^{(2)}|$, $\delta e_P = |e_P^{(1)} - e_P^{(2)}|$, and $\delta \sin i_P = |\sin i_P^{(1)} - \sin i_P^{(2)}|$. The indices (1) and (2) denote the two bodies under consideration. The C_a, C_e, and C_i are constants. We use $C_a = 5/4$, $C_e = 2$, and $C_i = 2$ (Zappalà et al. 1994). Other choices of these constants found in the literature yield similar results.
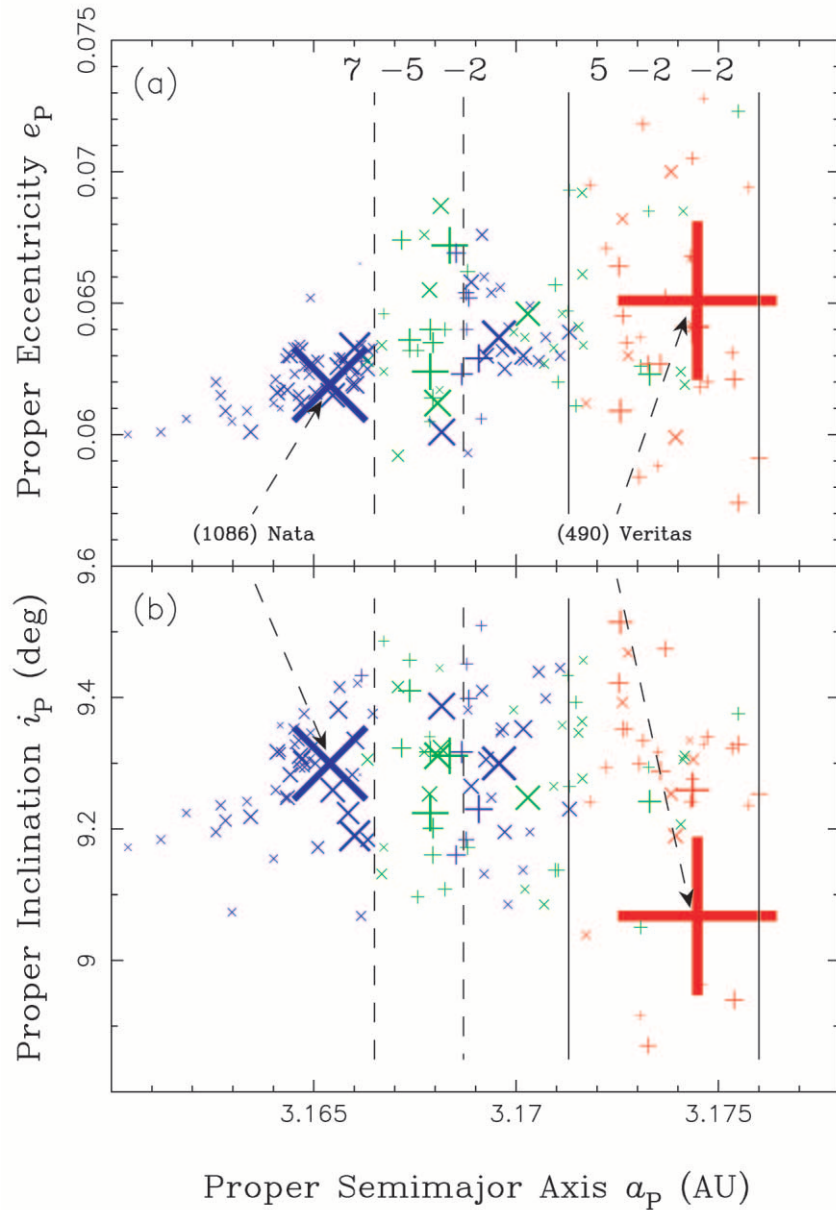
Fig. 2.—Proper orbital element distribution of Veritas family members: proper eccentricity vs. proper semimajor axis (*top*) and proper inclination vs. proper semimajor axis (*bottom*). The size of a symbol is proportional to asteroid size. The two largest bodies in the family, (490) Veritas (115 km diameter) and (1086) Nata (60 km diameter), are indicated by arrows. Colors denote Lyapunov times of orbits: $T_{\mathrm{Lyap}} < 10,000$ yr (*red*), $10,000$ yr $< T_{\mathrm{Lyap}} < 100,000$ yr (*green*), and $T_{\mathrm{Lyap}} > 100,000$ yr (*blue*). Two different symbols are used in the plot: crosses denote those orbits that show convergence of their nodal longitudes to a single value at 8.3 Myr ago, and plus signs denote the remaining orbits. The vertical lines delimit two major resonances located in the region: 5-2-2 (*right; solid lines*) and 7-5-2 (*left; dashed lines*) three-body resonances with Jupiter and Saturn (see Nesvorný & Morbidelli 1998). Note that regular nonresonant orbits (*blue*), whose past evolutions may be precisely reproduced by a numerical integrator, generally participate in the nodal conjunction 8.3 Myr ago.

used by Nesvorný et al. 2002a to identify the Karin cluster). The large semimajor axis end of the Veritas family, including (490) Veritas itself, appears to be more loosely connected with the rest of the family. This segregation may be the result of the chaotic 5-2-2 three-body resonance[4] (Nesvorný & Morbidelli 1998) that causes objects to quickly evolve in proper eccentricity and inclination at 3.172–3.176

AU. Similarly, the 7-5-2 three-body resonance may have dispersed family members at 3.166–3.169 AU. In order to highlight this resonant structure, we computed the Lyapunov times[5] (T_{Lyap}; see Benettin, Galgani, & Strelcyn 1976) of all family members. The colored points shown in Figure 2 denote the range of Lyapunov times we obtained: $T_{\mathrm{Lyap}} < 10,000$ yr (*red*), $10,000$ yr $< T_{\mathrm{Lyap}} < 100,000$ yr

---

[4] Three-body resonances are commensurabilities between the orbital motions of an asteroid and two planets. Three-body resonances with Jupiter and Saturn are common in the asteroid belt. The 5-2-2 three-body resonance is defined as $5n_{\mathrm{J}} - 2n_{\mathrm{S}} - 2n = 0$, where n_{J}, n_{S}, and n are the mean orbital frequencies of Jupiter, Saturn, and the asteroid, respectively.

[5] The maximum Lyapunov exponent measures the rate of divergence of nearby orbits and is a powerful indicator of chaos. It is mathematically defined as $\lim_{t\to\infty} \log \Delta(t)/t$, where $\Delta(t)$ is the norm of the variational vector at time t. The Lyapunov time (T_{Lyap}) is the inverse of the maximum Lyapunov exponent. The orbital evolution is unpredictable over time spans that significantly exceed T_{Lyap}.

(*green*), and $T_{\mathrm{Lyap}} > 100,000$ yr (*blue*). The Lyapunov times are nicely correlated with the background resonant structure. Most orbits with $T_{\mathrm{Lyap}} < 100,000$ yr, i.e., those characterized by rather strong chaotic behavior, are the resonant ones.

To determine the age of the Veritas family, we adopted the method of Nesvorný et al. (2002a). Immediately after the disruption, the cluster fragments all circled the Sun, as a group, in nearly identical orbits (differing only by small a, e, i values because of their modest ejection velocities). However, within $\sim$1000 yr, the objects drifted away from one another along their orbits (i.e., their true anomalies spread). Over longer timescales, planetary perturbations forced their orbital orientations (specified by the longitude of the ascending node and argument of perihelion) to drift away from each other, eventually spreading out uniformly around 360°. Thus, after a few million years, the once-clustered asteroids were spread into a dispersed toroid around the Sun. By numerically integrating the orbits of the Veritas family back in time until the orbital elements are clustered, we hope to find a conjunction of orbital elements, which should occur only in the immediate aftermath of the parent body disruption. This technique was successfully used in Nesvorný et al. (2002a) to determine the age of the Karin cluster (5.8 ± 0.2 Myr).

The Veritas family, however, is not quite as clear cut a case as the Karin cluster. While the Karin cluster was formed in a zone with few strong resonances, several powerful resonances exist in the 3.15–3.18 AU region. Hence, with the Veritas family overlapping these chaotic zones, only a fraction of the Veritas family members can be accurately integrated back in time. Moreover, Veritas family members are located close enough to the 2 : 1 mean motion resonance with Jupiter to undergo fast differential evolution of their arguments of perihelia. This induced variability in their evolution histories complicates any attempt to determine the age of the Veritas family from perihelion longitudes (such as was done for the Karin cluster; see Fig. 2*b* of Nesvorný et al. 2002a).

Instead, we have analyzed the past evolution of nodal longitudes of Veritas family members (equivalent to Fig. 2*a* of Nesvorný et al. 2002a) over a period of 50 Myr, omitting those objects that are evolving chaotically (i.e., that have short Lyapunov times). As shown in Figure 3, there is a conspicuous convergence of orbits $\sim$8.3 Myr ago, suggesting that the Veritas family was formed at that time. We estimate that the probability, over the age of the solar system, of so many asteroid orbits converging as tightly as they do in the Veritas family is less than 10^{-5}. Hence, we believe that it indeed represents another recent collisional disruption that occurred just a few million years before the Karin cluster formed.

We find this outcome to be something of a surprise because collisional disruption events among asteroids as large as $D \sim 140$ km (the scale of the Veritas precursor body; Table 1) are thought to be infrequent. Still, given the Veritas family age constraints provided by Milani & Farinella (1994) and Knežević et al. (2002b), we believe that this scenario is probably correct. On the other hand, it is also plausible that the conjunction of orbits was produced
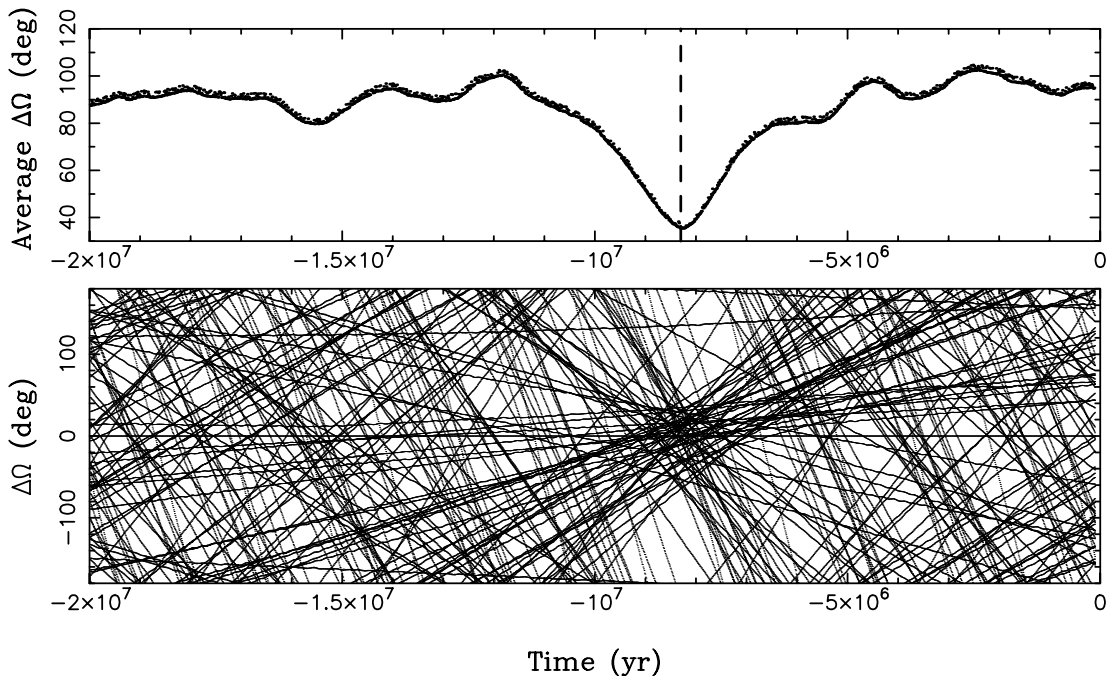

Fig. 3.—Convergence of nodal longitudes at $\approx$8.3 Myr suggests that a large part of the Veritas family formed by a catastrophic collision at that time. *Bottom:* Past orbital histories of nodal longitudes relative to (1086) Nata ($\Delta\Omega$). We show only those orbits that have $T_{\mathrm{Lyap}} > 100,000$ yr. *Top:* $\Delta\Omega$ averaged over these orbits. The average $\Delta\Omega$ is $\approx$40° at $t \sim -8.3$ Myr, much smaller than at other times. This suggests a statistical significance of the $t \sim -8.3$ Myr event. In this case, however, $\Delta\Omega$ values are substantially more spread at $t \sim -8.3$ Myr than in the Karin cluster at $t \sim -5.8$ Myr (Fig. 2*a* in Nesvorný et al. 2002a). This is primarily due to two reasons: (1) many chaotic resonances exist at 3.15–3.18 AU; thus, despite the present long Lyapunov times of the selected orbits, these orbits might have experienced periods of chaotic motion in the past; and (2) the Veritas family is more stretched over a_P than the Karin cluster; thus, some orbits have rather fast differential rotations with respect to the orbit of (1086) Nata, and small changes of their $d\Omega/dt$ (such as those generated by a semi-major axis drift due to the Yarkovsky effect) produce large effects. We do not show differential rotations of $\Delta\omega$ because these evolutions are too fast to be useful ($d\omega/dt$ has a large gradient at 3.15–3.18 AU due to the nearby 2 : 1 mean motion resonance with Jupiter).

TABLE 1
PROPERTIES OF SELECTED MAIN-BELT ASTEROID CLUSTERS

Cluster	d_{cutoff} (m s^{-1})	Number of Members	i_P (deg)	e_P	a_P (AU)	D_{PB} (km)	$M_{\text{LR}}/M_{\text{PB}}$	Taxonomic Type	Age (Myr)
832 Karin................	10	82	2.11	0.0445	2.866	27	0.37	S?	5.8
490 Veritas..............	40	259	9.26	0.0636	3.169	140	0.67	C	8.3
4652 Iannini............	30	18	12.17	0.2674	2.644	14[a]	0.22	...	≲5
3815 Konig	30	33	8.86	0.1395	2.572	32	0.46	C	[b,c]
1521 Seinajoki.........	40	78	15.02	0.1209	2.852	37[a]	0.26	...	[d]
13544 (606)[e]	20	27	9.61	0.1802	2.582	14[a]	0.10	K?	>15
396 Aeolia................	20	28	3.45	0.1681	2.741	36	0.92	Xe	>20
1400 Tirela[f]	40	44	16.89	0.1975	3.118	44[a]	0.24	...	[c,d]
845 Naema...............	40	64	11.96	0.0355	2.939	51	0.72	C	>20
1128 Astrid	50	65	0.68	0.0483	2.782	42	0.60	C	>20
1726 Hoffmeister......	30	181	4.38	0.0473	2.789	66	0.08	C	[g]20–250

[a] 12% albedo assumed; Bowell et al. 1989.

[b] Secular resonance $s - s_6 - g_5 + g_6 = 0$; Milani & Knežević 1994.

[c] Chaos from overlapping mean motion resonances; Nesvorný & Morbidelli 1998.

[d] Fast differential precession of nodes and apses.

[e] 606 Brangane joins at 30 m s^{-1} but is assumed to be an interloper here.

[f] Synthetic proper elements used; Knežević et al. 2002a.

[g] The upper age limit determined as in Fig. 4.

by a breakup of a smaller family member within the Veritas family. If this is true, this subcluster, formed only ~8.3 Myr ago, would have produced (1086) Nata and the other Veritas family members that contribute to the conjunction shown in Figure 3.

We believe that this collisional disruption event also produced the outer dust band. The mean proper inclination of the Veritas family ($i_P = 9°.3$) nearly equals the model-derived source inclination of the outer band ($i_P = 9°.35$). Moreover, the semimajor axis of the Veritas family (3.17 AU) is within the range of parallactic distances 3.2 ± 0.3 AU computed for the outer band by Reach et al. (1997). The large size of a parent body that disrupted 8.3 Myr ago also explains why the computed cross-sectional area of the outer dust belt is substantially larger than those of the central dust bands.

3.3. 1°.43 Dust Band

The provenance of the 1°.43 dust band is less clear. We have extensively searched for young collisional remnants with $i_P \sim 1°.43$ but find none. Ironically, two broadly diffused families are located at these inclinations: the Themis family, generally thought to be the source region of the 1°.43 dust band, and the Massalia family in the inner main belt. The mean proper inclinations of these families are 1°.40 and 1°.43, respectively. The Themis family formed by a catastrophic disruption of an ≈369 km diameter parent body (Tanga et al. 1999). Assuming that Themis family members have been significantly spread in semimajor axis via the Yarkovsky effect (see Bottke et al. 2001), we estimate that this family was created 2.5 ± 1.0 Gyr ago (Fig. 4a). This estimate assumes that the ejection velocities of family members were comparable to values produced by recent computer models (see Michel et al. 2001).

The Massalia family contains one large body [(20) Massalia, ≈145 km diameter] and a large number of 1–4 km diameter members. Because the small family members represent only ≈10% of the parent body's mass (Tanga et al. 1999), this family probably formed via a subcatastrophic collision. Given the limited semimajor axis spread of

Massalia family members, we believe that the Massalia family is significantly younger than the Themis family (i.e., according to our estimates, the Massalia family is 300 ± 100 Myr old; Fig. 4b).

It is unclear which of these two families is a better candidate for the source of the 1°.43 dust band. Our preferred scenario is that there was a recent disruption event within one of the two families. The Themis and Massalia families contain more known asteroids with $i_P \sim 1°.43$ than the rest of the main belt combined, making it likely that a recent disruption event could have occurred within one of them. Both families have high proper eccentricities (0.15 and 0.16, respectively), which place them in locations where mean motion resonances cause fast chaotic evolutions of orbits (see Nesvorný et al. 2002b). If some family member recently disrupted at such a location (an event similar to the formation of the Karin cluster in the Koronis family), the initially compact cluster of fragments produced by this disruption would rapidly disperse, leaving it unrecognizable by our algorithms after ≳10 Myr. This scenario would explain why we have been unable to find a recent source of this dust band. In fact, although we find about 10 unrelated very compact families in the central part of the belt (some of them are visible in Fig. 1), we find none in the inner main belt ($a_P < 2.5$ AU)[6] nor, with the exception of the Veritas family and (1400) Tirela (see next section), in the outer part of the main belt ($a_P > 2.95$ AU). This may reflect different degrees of dynamical erosion in the inner and outer parts of the main belt, where small collisional families rapidly disperse (see Nesvorný et al. 2002c).[7]

---

[6] Except the Massalia family region. Part of the Massalia family around (4579) Puccini ($a_P \sim 2.38$ AU) clusters at $d_{\text{cutoff}} = 30$ m s^{-1}. Unfortunately, orbital chaos due to the mean motion resonances with Mars (Morbidelli & Nesvorný 1999) prevents age determination for this cluster.

[7] On the other hand, it may also reflect the fact that collisional lifetimes are shorter by a factor of several in the central main belt; lifetimes against catastrophic disruption in the inner and outer main belt are generally longer because asteroids in those zones cross a smaller portion of the main-belt population (Bottke et al. 1994).
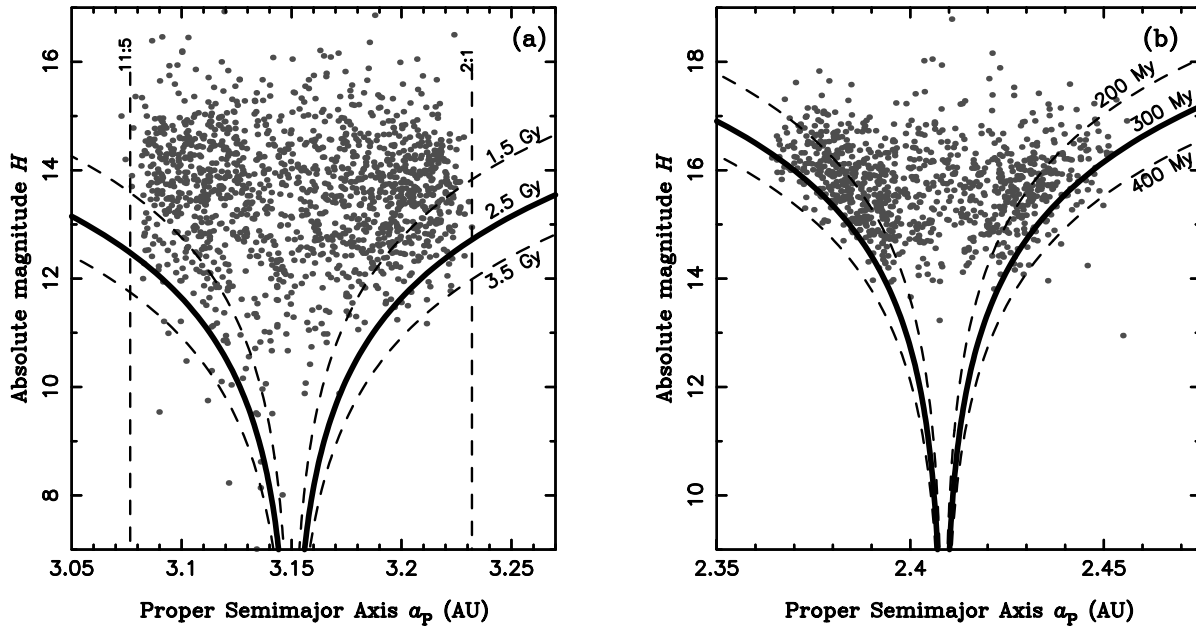
Fig. 4.—Absolute magnitudes (H) and proper semimajor axes (a_P) of (*a*) Themis and (*b*) Massalia family members (*dots*). The V-shaped lines indicate positions of Yarkovsky-drifting bodies evolved from the center of the families over the indicated time intervals, assuming maximum drift rates inward and outward. The drift rates were computed analytically using linearized approximations of the Yarkovsky effect (Vokrouhlický 1999). Assuming a tight initial orbital distribution of a newly born family, the family members are expected to be localized within one of the V-shaped contours. In (*a*), the distribution in a_P of the Themis family members with $H \gtrsim 12.5$ is cut by the chaotic 11 : 5 and 2 : 1 mean motion resonances with Jupiter. Using members with $H \lesssim 12.5$, we estimate that the Themis family is 2.5 ± 1.0 Gyr old. From (*b*), the Massalia family is 300 ± 100 Myr old. These estimates are robust over a wide range of the physical parameters compatible with the family's taxonomic type (Themis is C; Massalia is S) and with asteroidal surfaces covered by regolith. The outliers shown in the figure are probably interlopers.

For these reasons, the origin of the 1°43 dust band is less clear. Interestingly, the Themis family, located at the same inclination, is the remnant of one of the largest catastrophic disruption events (that we have evidence for) in the asteroid belt. The amount of dust generated by the comminution of Themis's early fragments must have been staggering, such that it is plausible that, even after ~2 Gyr, there may still be enough collisional activity taking place to create a detectable dust band (Sykes & Greenberg 1986).

3.4. *Other Dust Bands and Clusters*

To identify the possible source regions of the E/F, G/H, J/K, and M/N dust bands (Sykes 1990; Reach et al. 1997), we searched the main belt for additional compact (i.e., possibly young) asteroid families. Once again, we applied the HCM (Zappalà et al. 1994) with cutoffs $d_{cutoff} = 20$–50 m s^{-1} to a recent database of $\approx 100,000$ proper elements found at the AstDys node (Milani & Knežević 1994; Knežević et al. 2002a). To find an appropriate d_{cutoff} for each cluster, we developed an interactive visualization program that allowed us to "browse" asteroid proper element space. Using this program, we inspected the three-dimensional structure of each cluster and chose the d_{cutoff} value that provided the best visible match.

In all, we identified 28 tightly clustered asteroid families in the main-belt region, most of which were previously unknown. Of this set, the Karin cluster, the Veritas family, and nine other groups were compact enough to make us believe that they were probably generated by collisions within the last ~100 Myr. In this section, we will concentrate on analyzing these groups. The remaining 17

structures[8] bear the marks of dynamical erosion over longer timescales (probably $\gtrsim 100$ Myr). Because they are less probable dust band sources, we will not discuss them further in this paper.

Table 1 shows properties of the nine new compact clusters. Columns give the lowest numbered cluster member, cutoff distance used (d_{cutoff}), number of members at this d_{cutoff}, average proper elements, parent body diameter (D_{PB}), largest remnant's mass to parent body's mass ratio (M_{LR}/M_{PB}), taxonomic type (Bus & Binzel 2002), and estimated age of the cluster. To convert magnitudes H to diameters, we used the albedo of the largest cluster members, if known, or 12% albedo otherwise (Bowell et al. 1989). Here D_{PB} is the diameter of a spherical body with volume equal to the total volume of all known cluster members.

To determine the age of a cluster, we numerically integrated the member asteroids' orbits backward in time to check whether any nodal or apsidal alignments occur (Nesvorný et al. 2002a; our Fig. 3). This method has, however, fundamental limitations. It is impossible to correctly reproduce the past evolution of Ω and ω for those cluster members that have strongly chaotic orbits. For example, members of the cluster around (1400) Tirela have orbits that have been strongly affected by chaotic mean motion resonances with Jupiter (Nesvorný & Morbidelli 1998).

---

[8] Clustered around (3) Juno, (87) Sylvia, (128) Nemesis, (283) Emma, (298) Baptistina, (363) Padua, (569) Misa, (668) Dora, (808) Merxia, (847) Agnia, (2980) Cameron, (3556) Lixiaohua, (4130) Ramanujan, (4579) Puccini, (5026) Martes, (9506) Telramund, and (18405) 1993 FY12.
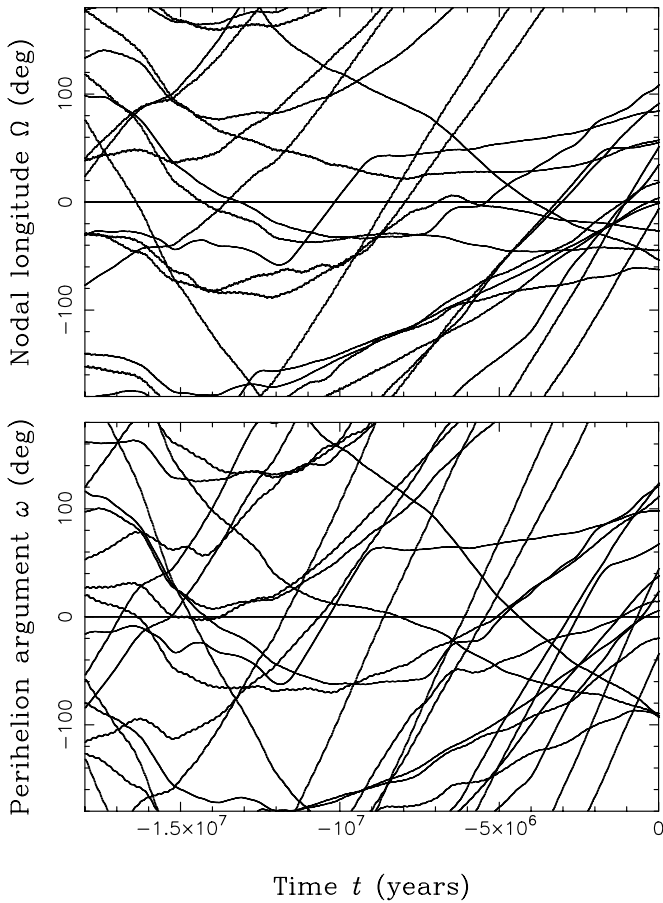
FIG. 5.—Members of the (4652) Iannini cluster have a nonuniform distribution of Ω and ω at $t = 0$ (today). This distribution only persists over a few Myr into the past, indicating that the (4652) Iannini cluster is probably $\lesssim 5$ Myr old. If this were not the case, we would be unable to see the signature of the initial alignment of secular angles at $t = 0$. The chaotic evolution of secular angles is induced by numerous overlapping mean motion resonances with Mars (Morbidelli & Nesvorný 1999).

Consequently, we were unable to determine this cluster's age by a backward integration.

For one cluster, however, we were able to set an upper limit on its age despite the strongly chaotic evolution of its members. The members of the (4652) Iannini cluster currently have a significantly nonuniform distribution of Ω and ω. In fact, all 18 members of this cluster currently have $\Omega \in (245°, 75°)$ and $\omega \in (285°, 157°)$; i.e., Ω and ω are distributed within only 53% and 64% of the full 360° interval, respectively. Our backward integration shows that this concentrated distribution of nodes and apses persists for only a few Myr (Fig. 5). For $t \lesssim -5 \times 10^6$ yr, nodes and apses become random. Moreover, the currently observed concentration of Ω and ω never repeats over the age of the solar system. Based on this information, we estimate that the (4652) Iannini cluster was created by a disruptive collision over the last $\lesssim 5$ Myr.

(3815) Konig is another chaotic cluster that displays a peculiar concentration of secular angles; 27 of its 33 members have Ω values that are strongly concentrated around $0°$. In this case, however, the concentration is not a signature of the young age of the cluster but was instead generated by the secular resonance $s - s_6 - g_5 + g_6 = 0$ (Milani

& Knežević 1994).[9] Although the Konig cluster's compact orbital structure in the (a_P, e_P, i_P) space could still be a by-product of its recent origin, we are currently unable to determine its exact age.

Yarkovsky thermal drag forces (e.g., Bottke et al. 2002) also complicate our method of determining cluster ages. The Yarkovsky effect causes objects to drift in semimajor axis, with a direction and magnitude that strongly depends on the body's obliquity ϵ (the angle between the body's spin axis and the normal to the orbital plane). For $\epsilon = 0$ (prograde rotation) the body evolves to larger a_P values, while for $\epsilon = 180°$, the body evolves to smaller a_P values. These changes in a_P may eventually spread some clusters enough that they become indistinguishable from the background. Thus, Yarkovsky spreading timescales place limits on the *detectability* of the cluster. Over shorter time spans, Yarkovsky drift modifies the precession rates of the secular angles in a manner that cannot be predicted unless we first know ϵ. Because ϵ is unknown for most asteroids, we cannot compute the cluster's age unless it is younger than the timescale over which secular angles are significantly affected by Yarkovsky drift. We call this limit the age computability threshold.

Because the Yarkovsky effect is a size-dependent force, both the cluster detectability and age computability limits depend on the size of member asteroids of any given cluster. Figure 6 shows both limits as a function of this size. We define the age computability limit ($\tau_{\rm AC}$) as the time horizon at which the majority of cluster members drift far enough in a_P to induce changes that spread Ω over $\pm\pi/2$ around a nondrifting orbit. Note that $d\omega/dt$ in the main-belt region is more sensitive to changes in a_P than $d\Omega/dt$, such that members' apses are expected to randomize over a shorter interval than $\tau_{\rm AC}$. Still, age determination is possible within $\tau_{\rm AC}$ if one concentrates on the past evolution of the nodes.

We calculate $\tau_{\rm AC}$ from

$$\tau_{\rm AC} = \sqrt{\frac{\pi}{(\partial s/\partial a_P)\langle da_P/dt\rangle_{\rm Y}}} \,, \qquad (1)$$

where $\langle da_P/dt\rangle_{\rm Y}$ is the average rate of drift induced by the Yarkovsky effect and

$$\frac{\partial s}{\partial a_P} = \frac{9}{8}\frac{GM_{\rm J}}{\sqrt{GM_\odot}}\frac{a_P^{1/2}}{a_{\rm J}^3}\left(1 + \frac{35}{8}\frac{a_P^2}{a_{\rm J}^2}\right). \qquad (2)$$

This last equation describes how the rate of nodal precession s induced by Jupiter changes with a_P (e.g., Sykes & Greenberg 1986). G, $M_{\rm J}$, and $M_\odot$ are the gravitational constant, mass of Jupiter, and mass of the Sun, respectively, and $a_{\rm J} \sim 5.2$ AU is the average distance of Jupiter from the Sun. We calculate $\langle da_P/dt\rangle_{\rm Y}$ from the linear theory of the Yarkovsky effect for spherical bodies covered by regolith (Vokrouhlický 1999). Figure 6 shows $\tau_{\rm AC}$ as a function of the cluster members' sizes.

We define the cluster detectability limit ($\tau_{\rm CD}$) as the time interval over which the majority of cluster members move Δa_P via the Yarkovsky effect:

$$\tau_{\rm CD} = \frac{\Delta a_P}{\langle da_P/dt\rangle_{\rm Y}} \,, \qquad (3)$$

[9] Here s is the mean rate of the nodal precession of an asteroid and $s_6 = -26{.}''34$ yr^{-1}, $g_5 = 4{.}''26$ yr^{-1}, and $g_6 = 28{.}''25$ yr^{-1} are the secular frequencies of the planetary system (e.g., Laskar 1988).
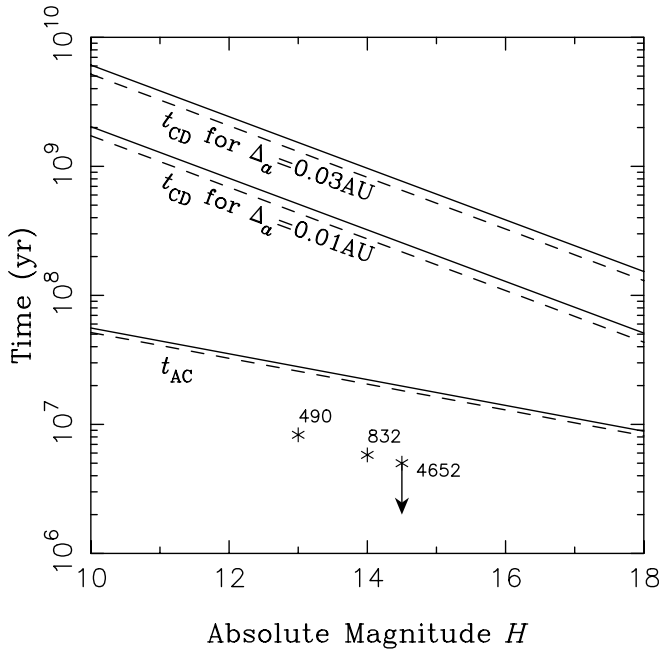
FIG. 6.—Age computability (t_{AC}) and cluster detectability (t_{CD}) thresholds as a function of the absolute magnitude of asteroid members in a cluster. The solid and dashed lines correspond to S and C taxonomic types. We find little difference between C-type and S-type objects; C-type objects of a given H are about twice as large ($\sim$5% albedo) as the same-H S-type objects ($\sim$15% albedo), but they are also nearly twice as low in density (e.g., Britt et al. 2002). Consequently, the thresholds are similar because the Yarkovsky drift rates are similar (Vokrouhlický 1999). We plot two values of t_{CD} that correspond to smaller (0.01 AU) and larger (0.03 AU) semimajor axis drift rates that lead to cluster erasure. Asterisks mark locations of the clusters with known ages: (490) Veritas, (832) Karin, and (4652) Iannini. Note that these ages are less than t_{AC}, as expected.

where Δa_P is some multiple of the cluster's original size in a_P (i.e., the spread produced by the fragments' ejection velocities). Because all of our identified clusters with $D_{PB} \lesssim 50$ km are spread over $\lesssim 0.03$ AU (Fig. 1), we believe that $\Delta a_P \lesssim 0.03$ AU is an appropriate choice. Figure 6 shows τ_{CD} for $\Delta a_P = 0.01$ and 0.03 AU. We point out that τ_{CD} does not account for other effects that may erase asteroid families such as chaos (Nesvorný et al. 2002c) or the collisional grinding of family members down to small, unobservable sizes (Marzarii, Farinella, & Davis 1999).

Figure 6 shows that recent breakups such as those that produced the Karin cluster and the Veritas family should be detectable even after $\tau_{CD} \sim 5 \times 10^8$ yr (unless they get erased earlier by chaotic dispersal or collisions). Their age, however, can be computed only provided they are younger than $\tau_{AC} \sim 2 \times 10^7$ yr. This explains why we were unable to calculate ages for most clusters shown in Table 1 by a backward integration over $\sim \tau_{AC}$. These clusters must be older than τ_{AC} but younger than τ_{CD}.

The clusters around (1521) Seinajoki and (1400) Tirela have large i_P values ($\sim$15° and $\sim$17°, respectively) and are spread enough in a_P that the differential nodal (and apsidal) precession of their members is fast. It is difficult to determine the age of these clusters by backward integration because individual paths of Ω and ω densely fill the 360° interval. For this reason, we cannot exclude the possibility that (1521) Seinajoki and (1400) Tirela are younger than τ_{AC}.

For most of the remaining clusters with slow differential precession rates, we detected no alignment of secular angles

within τ_{AC} (last column in Table 1). For this reason, we were able to set a minimum age threshold by integrating their members' orbits backward in time.

3.4.1. *M/N Dust Band*

Based on the inclination fit in Figure 1, we tentatively associate the M/N dust band (Sykes 1990) with the cluster of asteroids located around (1521) Seinajoki. This cluster was previously known as a marginally significant asteroid grouping found around (293) Brasilia ($\approx$110 km in diameter). Using the new catalog of the proper elements described above, we find that (293) Brasilia is located on the periphery of the newly determined cluster (i.e., the HCM cluster shows that it is separated from the rest of the family members by $d_{cutoff} \sim 60$ m s^{-1}). The family currently contains $\approx$80 members at the 40 m s^{-1} level with absolute magnitudes $11 < H < 16$. Although this family's compact structure in proper element space suggests that it is young, we were unable to determine its age for the reasons discussed above.

The M/N dust band was previously associated with the Maria family, whose members cluster near $\sim$15° inclination (Reach et al. 1997). From Figure 1, it appears that parts of the Maria family are as dense as the (1521) Seinajoki cluster in (a_P, e_P, i_P). This ignores the fact, however, that the Maria family is spread over 0.08 in e_P while the (1521) Seinajoki cluster is spread over only 0.006 in e_P. Hence, the Maria family only looks dense in Figure 1, where three-dimensional space is projected into the (a_P, i_P) plane. In reality, there are no compact structures within its boundaries even at $d_{cutoff} \sim 50$ m s^{-1} levels.

3.4.2. *J/K Dust Band*

The J/K dust band was previously associated with the Eunomia family (Sykes 1990; Reach et al. 1997), which is a widely dispersed and probably billions of years old structure in the central main belt ($a_P \sim 2.6$ AU). Reach et al. (1997), however, found a substantially lower inclination for the source region of this dust band ($i_P = 12°11$) than the mean inclination of the Eunomia family ($i_P = 13°1$). This situation is reminiscent of the inclination offset found between the γ–dust band and the Eos family (see § 3.2).

There are two candidates for the J/K dust band source region among the compact asteroid clusters: (4652) Iannini and (845) Naema ($i_P = 12°17$ and $i_P = 11°96$, respectively). For the cluster around (4652) Iannini, we estimate its age to be $\lesssim 5$ Myr, while the cratering event ($M_{LR}/M_{PB} \sim 0.72$; Table 1) that formed the (845) Naema cluster occurred more than 20 Myr ago. We thus believe that the more recent breakup of the (4652) Iannini cluster's parent body ($D_{PB} \sim 14$ km) is the best candidate for being the ultimate source of the J/K dust band. This cluster is difficult to see in Figure 1 because its 18 members are projected on the main-belt background. It is nevertheless statistically significant and readily detectable by both the HCM and our three-dimensional visualization browser.

3.4.3. *E/F and G/H Dust Bands*

Neither Nysa/Polana nor Flora, the prominent asteroid families in the inner main belt (Zappalà et al. 1994), can be linked to the E/F and G/H dust bands, which are the two pairs of dust bands located at latitudes between the β– and γ–dust bands (Sykes 1990). We also find no other known large asteroid families at the corresponding inclinations

(between $\sim 3°$ and $\sim 9°$). Reach et al. (1997) found that the parent families of these bands should have a relatively sharp proper inclination distribution. We found three tightly grouped asteroid clusters at the corresponding inclinations: (396) Aeolia, (1726) Hoffmeister, and (3815) Konig (Table 1). None of these clusters, however, seems to be younger than 20 Myr.

4. DISCUSSION

We have argued in this paper that the *IRAS* dust bands are by-products of recent collisions among main-belt asteroids. In particular, we proposed that the brightest "outer" (or γ) dust band was produced by the formation of the Veritas family. Our results suggest that this event occurred 8.3 ± 0.5 Myr ago. Our scenario matches all basic constraints imposed by observations and modeling work performed on the outer dust band. Similarly, we find it likely that the formation of the Karin cluster 5.8 ± 0.2 Myr ago led to the formation of the 2°.1 (or β) dust band.

Physical studies of the interplanetary dust particles accreted by the Earth, and spectral observations of the Veritas family, may be consistent with our suggested links:

1. Di Martino et al. (1997) noted spectral differences in the Veritas family spanning taxonomic types from C to D type. Based on these results, Di Martino et al. suggested that the parent body of the Veritas family was a differentiated object. (1086) Nata, (1985) TQ1, and (2934) Aristophanes, all located in the tight cluster at $a_P < 3.1665$ AU in Figure 2, have very flat spectra typical for C types with a shallow and wide absorption band centered at 7000 Å. Di Martino et al. attributed this absorption band to aqueous alteration near the surface of the parent body. According to their interpretation, (490) Veritas, which does not show the same feature, may be the core of the parent body. This spectral diversity among the Veritas family members is unique (other asteroid families are more homogeneous) and may be a signature of its young age.

2. On the other hand, Dermott et al. (2002) argued that about 25% of the IDPs collected by airborne impaction collectors flown in the Earth's stratosphere sample material from the outer dust band. Mineralogical and chemical composition overlaps between IDPs and micrometeorites (MMs, $\gtrsim 50$ μm particles collected in the Antarctic and Greenland). Moreover, MMs (and IDPs) bear similarities to the CI/CM/CR carbonaceous chondrites (Jessberger et al. 2001). CI/CM chondrites that suffered aqueous alteration are especially similar to C-type asteroids (McSween 1979).

To our knowledge, the predominantly C-type Veritas family is the best candidate for the origin of (some part of) the CS IDPs. It would be interesting to obtain visible and infrared spectra of a large number of Veritas family members and compare them to the known spectra of the IDPs. If some characteristic spectral features are shared by both samples, it would further support our scenario for the origin of the outer dust band.

Our hypothesis is also testable by measurements of the extraterrestrial ^{3}He in $\lesssim 10$ Myr old geological layers on the Earth. The flux of ^{3}He is a proxy for the terrestrial accretion rate of IDPs (Farley et al. 1998; Mukhopadhyay, Farley, & Montanari 2001). If our hypothesis is correct, we would expect an enhanced abundance of ^{3}He in ~ 8.3 Myr layers (the time when Veritas/Nata family formed). Similarly, a somewhat weaker signature at ~ 5.8 Myr could have been produced by the Karin cluster formation.

We were unable to identify a recent disruption event in the main-belt region that could be responsible for the 1°.4 dust band. An event within the Themis family, which is the remnant of one of the largest single catastrophic disruption events (for which we have evidence) in the asteroid belt, remains the best candidate for the 1°.4 dust band source region. The smaller and younger Massalia family in the inner main belt is also located at $i_P \sim 1°.4$. We point out that it is challenging to find remnants of recent disruptions in the Themis and Massalia families because tight clusters in (a_P, e_P, i_P) space at the main-belt locations of these families rapidly disperse by chaotic effects.

We speculate that the (4652) Iannini cluster ($\lesssim 5$ Myr old, $i_P \sim 12°$) is the source for the J/K dust band and that the (1521) Seinajoki cluster ($\sim 15°$ inclination) is the ultimate source for the M/N dust band. If recent breakups, rather than old and prominent asteroid families, are responsible for the observed dust bands, these associations can explain why previous models had some difficulty matching the spatial distribution of these weaker dust bands.

Finally, our scenario also explains why many large asteroid families (such as Flora, Nysa/Polana, Vesta, Hygiea, etc.) do not have associated dust bands. Most of these families are ancient, such that any dust produced by their formation is long gone today. The total surface area of the dust produced in the aftermath of these events via a collisional cascade declined over long timescales because there are generally not enough collisions among family members to keep their associated dust bands from slowly fading away. Sykes & Greenberg (1986) have shown, however, that the observable signal is most likely reduced by orders of magnitude after billions of years of evolution. It is thus conceivable that most old asteroid families do not contribute in any significant fashion to the main-belt dust population observed today.

REFERENCES

Bendjoya, Ph., & Zappalà, V. 2002, in Asteroids III, ed. W. F. Bottke et al. (Tucson: Univ. Arizona Press), 613
Benettin, G., Galgani, L., & Strelcyn, J. M. 1976, Phys. Rev. A, 14, 2338
Benz, W., & Asphaug, E. 1999, Icarus, 142, 5
Bottke, W. F., Nolan, M. C., Greenberg, R., & Kolvoord, R. A. 1994, Icarus, 107, 255
Bottke, W. F., Vokrouhlický, D., Brož, M., Nesvorný, D., & Morbidelli, A. 2001, Science, 294, 1693
Bottke, W. F., Vokrouhlický, D., Rubincam, D. P., & Brož, M. 2002, in Asteroids III, ed. W. F. Bottke et al. (Tucson: Univ. Arizona Press), 395

Bowell, E., Hapke, B., Domingue, D., Lumme, K., Peltoniemi, J., & Harris, A. W. 1989, in Asteroids II, ed. T. Gehrels (Tucson: Univ. Arizona Press), 524
Britt, D. T., Yeomans, D., Housen, K., & Consolmagno, G. 2002, in Asteroids III, ed. W. F. Bottke et al. (Tucson: Univ. Arizona Press), 485
Burns, J. A., Lamy, P. L., & Soter, S. 1979, Icarus, 40, 1
Bus, S. J., & Binzel, R. P. 2002, Icarus, 158, 146
Davis, D. R., Chapman, C. R., Greenberg, R., & Weidenschilling, S. J. 1979, in Asteroids, ed. T. Gehrels (Tucson: Univ. Arizona Press), 528

Davis, D. R., Durda, D. D., Marzari, F., Campo Bagatin, A., & Gil-Hutton, R. 2002, in Asteroids III, ed. W. F. Bottke et al. (Tucson: Univ. Arizona Press), 545

Dermott, S. F., Durda, D. D., Grogan, K., & Kehoe, T. J. J. 2002, in Asteroids III, ed. W. F. Bottke et al. (Tucson: Univ. Arizona Press), 423

Dermott, S. F., Nicholson, P. D., Burns, J. A., & Houck, J. R. 1984, Nature, 312, 505

Di Martino, M., Migliorini, F., Zappalà, V., Manara, A., & Barbieri, C. 1997, Icarus, 127, 112

Durda, D. D., & Dermott, S. F. 1997, Icarus, 130, 140

Farley, K. A., Montanari, A., Shoemaker, E. M., & Shoemaker, C. S. 1998, Science, 280, 1250

Fujiwara, A., Cerroni, P., Davis, D., Ryan, E., & di Martino, M. 1989, in Asteroids II, ed. T. Gehrels (Tucson: Univ. Arizona Press), 240

Grogan, K., Dermott, S. F., & Durda, D. D. 2001, Icarus, 152, 251

Grün, E., Fechtig, H., Zook, H. A., & Giese, R. H. 1985, in IAU Colloq. 85, Properties and Interactions of Interplanetary Dust, ed. R. H. Giese & P. L. Lamy (Dordrecht: Reidel), 411

Hirayama, K. 1918, AJ, 31, 185

Holsapple, K., Giblin, I., Housen, K., Nakamura, A., & Ryan, E. 2002, in Asteroids III, ed. W. F. Bottke et al. (Tucson: Univ. Arizona Press), 443

Ishiguro, M., Nakamura, R., Fujii, Y., & Mukai, T. 1999, ApJ, 511, 432

Jessberger, E. K., et al. 2001, in Interplanetary Dust, ed. E. Grün et al. (Berlin: Springer), 253

Kehoe, T. J. J., Dermott, S. F., & Grogan, K. 2001, AAS Meeting, 32, 01.05

Keller, L. P., Thomas, K. L., & McKay, D. S. 1993, Meteoritics, 28, 378

Klöck, W., & Stadermann, F. J. 1994, in AIP Conf. Proc. 310, Analysis of Interplanetary Dust, Proc. NASA/LPI Workshop, ed. E. Zolensky et al. (New York: AIP), 51

Knežević, Z., Lemaitre, A., & Milani, A. 2002a, in Asteroids III, ed. W. F. Bottke et al. (Tucson: Univ. Arizona Press), 603

Knežević, Z., Tsiganis, K., & Varvoglis, H. 2002b, in Asteroids, Comets, and Meteors, ed. B. Warmbeim (ESA SP-500; Noordwijk: ESA), 52

Laskar, J. 1988, A&A, 198, 341

Love, S. G., & Brownlee, D. E. 1993, Science, 262, 550

Low, F. J., et al. 1984, ApJ, 278, L19

Marzari, F., Davis, D., & Vanzani, V. 1995, Icarus, 113, 168

Marzari, F., Farinella, P., & Davis, D. R. 1999, Icarus, 142, 63

McSween, H. Y. 1979, Rev. Geophys. Space Phys., 17, 1059

Michel, P., Benz, W., Tanga, P., & Richardson, D. 2001, Science, 294, 1696

Milani, A., & Farinella, P. 1994, Nature, 370, 40

Milani, A., & Knežević, Z. 1994, Icarus, 107, 219

Morbidelli, A., & Nesvorny, D. 1999, Icarus, 139, 295

Mukhopadhyay, S., Farley, K. A., & Montanari, A. 2001, Geochim. Cosmochim. Acta, 65, 653

Nakamura, A., Suguiyama, K., & Fujiwara, A. 1992, Icarus, 100, 127

Nesvorný, D., Bottke, W. F., Dones, L., & Levison, H. F. 2002a, Nature, 417, 720

Nesvorný, D., Ferraz-Mello, S., Holman, M., & Morbidelli, A. 2002b, in Asteroids III, ed. W. F. Bottke et al. (Tucson: Univ. Arizona Press), 379

Nesvorný, D., & Morbidelli, A. 1998, AJ, 116, 3029

Nesvorný, D., Morbidelli, A., Vokrouhlický, D., Bottke, W. F., & Brož, M. 2002c, Icarus, 157, 155

Reach, W. T. 1992, ApJ, 392, 289

Reach, W. T., Franz, B. A., & Weiland, J. L. 1997, Icarus, 127, 461

Spiesman, W. J., et al. 1995, ApJ, 442, 662

Sykes, M. V. 1988, ApJ, 334, L55

———. 1990, Icarus, 85, 267

Sykes, M. V., & Greenberg, R. 1986, Icarus, 65, 51

Sykes, M. V., Lebofsky, L. A., Hunten, D. M., & Low, F. J. 1986, Science, 232, 1115

Tanga, P., Cellino, A., Michel, P., Zappalà, V., Paolicchi, P., & Dell'Oro, A. 1999, Icarus, 141, 65

Vickery, A. M. 1993, Icarus, 105, 441

Vokrouhlický, D. 1999, A&A, 344, 362

Williams, J. G. 1992, Icarus, 96, 251

Zappalà, V., Cellino, A., Dell'Oro, A., & Paolicchi, P. 2002, in Asteroids III, ed. W. F. Bottke et al. (Tucson: Univ. Arizona Press), 619

Zappalà, V., Cellino, A., Farinella, P., & Milani, A. 1994, AJ, 107, 772

Zook, H. A., & Berg, O. E. 1975, Planet. Space Sci., 23, 183